Convertible Bandstop to Allpass Filter using Defected Ground Structure with Ideal Switch for Millimeter-Wave Band in 5G Application

Adib Othman[1], Huda A Majid[1*], Noor Azwan Shairi[2], Najib Al-Fadhali[1], Imran Mohd Ibrahim[2], Zahriladha Zakaria[2], Zuhairiah Zainal Abidin[1], Mohamad Kamal A Rahim[3], Bashar Ali F Esmail[4]

[1]Fakulti Teknologi Kejuruteraan,
 Universiti Tun Hussein Onn Malaysia, Pagoh Higher Education Hub, Pagoh, Muar, Johor, 84600, MALAYSIA

[2]Fakulti Kejuruteraan Elektronik dan Kejuruteraan Komputer,
 Universiti Teknikal Malaysia Melaka, Hang Tuah Jaya, Durian Tunggal, Melaka, 76100, MALAYSIA

[3]Fakulti Kejuruteraan, Sekolah Kejuruteraan Elektrik,
 Universiti Teknologi Malaysia, Skudai, Johor Bahru, Johor, 81310, MALAYSIA

[4]Department of Engineering,
 Reykjavik University, Reykjavik, 102, ICELAND

*Corresponding Author

Abstract: According to this study, a defective ground structure (DGS) with an ideal switch can be used to create a bandstop to allpass filter for 5G applications. The redesigned Hairpin DGS's bandstop and allpass responses are mathematically investigated in this paper. Utilising an ideal switch via open circuit and short circuit conditions on DGS, the convertible filter is operated. Therefore, the filter's performance in terms of return loss, attenuation, and insertion loss is simulated. As a result, the filter operates at 25.875 GHz in open circuit condition with a narrowband (2.16 GHz) bandstop response at 10 dB and a maximum attenuation of 29.5 dB, and at 26 GHz with a wideband allpass response and return loss greater than 10 dB. As a result, the filter is appropriate for 5G applications that use millimeter-wave RF front-end systems.

Keywords: Defected ground structure, bandstop to allpass, convertible filter, millimeter-wave

1. Introduction

Wireless communication networks are now complex and dynamic as a result of the need for faster data rates as well as the assignment of the radio spectrum band at higher frequencies. This is demonstrated by the use of newly developed 5G technology in the millimeter-wave (mm-wave) spectrum [1]. The FSS satellite, however, experiences interruption via numerous IMT-2020s (5G communication standard) in the mm-wave frequencies, illustrated in [2], and therefore this novel approach will clash with today's technology.

A cognitive radio (CR) is therefore important for 5G mm-wave communications to minimise potential interruptions. As a consequence, there are numerous approaches to interference mitigation in CR systems, including spectrum sensing algorithms based on energy detection [3], collaborative spectrum detection for reducing interruption

as well as enhancing the utilisation of the unoccupied radio spectrum [4], multi-hop multiple input multiple output (MIMO) decode-and-forward transmitting processes [5], interruption management techniques for device-to-device (D2D) applications [6], and ultra-wideband.

Additionally, CR front-end systems need adaptable components like filters [8] and antennas [9] to enable multi-channel, multi-band, and multipurpose tasks while also providing an interference mitigation solution. To directly minimise interruption within the front-end receiver, this technique is referred to as active interruption rejection [7]. Therefore, as mentioned in [8] and [9], it is crucial to have a good network or system controlled via varactor or PIN diodes.

Research is being done on the utilisation of DGS in RF design for particular purposes or parameter alterations. DGS utilisation alters the microstrip line's directed wave characteristics, which change the propagation constant and produce responses that function as a bandstop filter [10]–[12]. DGS therefore has a lot of potential for increasing bandwidth, shrinking size, reducing insertion loss, and enhancing return loss [13]–[17].

In order to support mm-wave communications, such as 5G technology, a defective ground structure (DGS) with an ideal switch is presented in this study for the 26 GHz band. The filter was created for the CR system, specifically for use in the 26 GHz band for 5G communications. Additionally, a mathematical analysis for the transition between bandstop and allpass responses is presented and explored in this study.

2. Mathematical Analysis of DGS with Ideal Switch

A DGS corresponding circuit with an ideal switch that acts as a switching component within allpass and bandstop responses is displayed in Fig. 1. According to [18], the corresponding circuit for DGS is a straightforward parallel L and C. Consequently, the DGS impedance is given as

$$Z_{DGS} = jX_{LC} = \frac{\left(\frac{1}{j\omega C}\right)(j\omega L)}{\frac{1}{j\omega C} + j\omega L} = \frac{j\omega L}{1 - \omega^2 LC} \qquad (1)$$

Now take into account an OFF state, wherein the DGS ideally ought to be open circuited. As a consequence of this, the DGS performs like a bandstop. Next, the DGS's transmission matrix (ABCD) is

$$[T_{DGS}] = \begin{bmatrix} 1 & \dfrac{j\omega L}{1 - \omega^2 LC} \\ 0 & 1 \end{bmatrix} \qquad (2)$$

The bandstop response of S21 is determined by (2) utilising conversion between ABCD and S-parameters.

$$S_{21} = \frac{2}{2 + \dfrac{j\omega L}{\left(1 - \omega^2 LC\right)Z_0}} \qquad (3)$$

The transmission line of the DGS has a characteristic impedance known as Z_0. It is clear from (3) that the L and C components are responsible for the bandstop's notch if $Z_0 = 1$ which is a normalize impedance. After that, the DGS's resonance frequency can be discovered when

$$j\omega L - \frac{1}{j\omega C} = 0 \qquad (4)$$

Thus,

$$f_0 = \frac{1}{2\pi\sqrt{LC}} \qquad (5)$$

where f_0 is the resonant frequency in Hertz. The S_{21} in (3) at OFF state also determined by condition in (4) and thus becomes

$$S_{21} = \frac{2}{2 + \infty} = 0 = \infty \; dB \qquad (6)$$

It is clear from (6) that a bandstop response can be constructed with optimally high attenuation.
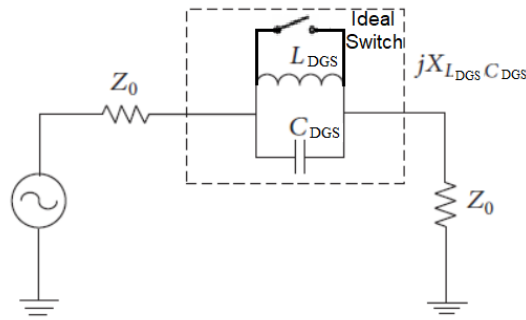

Fig. 1 - DGS circuit model with the ideal switch

The following analysis takes into account an ON state, where the DGS is meant to be shorted. The DGS responds as an allpass as a result. [18] asserts that the dumbbell DGS's rectangular portions improve effective inductance and current path length. In the meantime, the slot section builds up charge, thus raising the microstrip line's effective capacitance. The allpass response can therefore theoretically be formed if either of the two elements of L or C are zero. Given that the rectangular sections of the DGS were short-circuited in the ON state, L is zero, and let $Z_0 = 1$ thereby is a normalised impedance, then the S_{21} of (3) in the ON state becomes

$$S_{21} = \frac{2}{2 + 0} = 1 = 0 \, dB \qquad (7)$$

According to (7), an allpass response can be created with a perfect zero insertion loss.

Further research with respect to any electronic design automation (EDA) software is required for any type of DGS based on the mathematical analyses for the purpose of converting it among allpass and bandstop responses. The placement of the effective inductance and capacitance for ideal switches vary depending on the type of DGS.

3. DGS with Ideal Switch Design

The ideal switch notion is the foundation of the convertible DGS architecture. A short circuit condition (passive DGS) and an open circuit condition (active DGS) are the two main layouts for DGS. As shown in Fig. 2(a), the Hairpin DGS base from [19] is modified and hence depicted in Fig. 2(b) with a shorted copper sheet is added to the DGS, causing it to become in a short circuit condition. It must be modified in order for it to function in the mm-waveband.
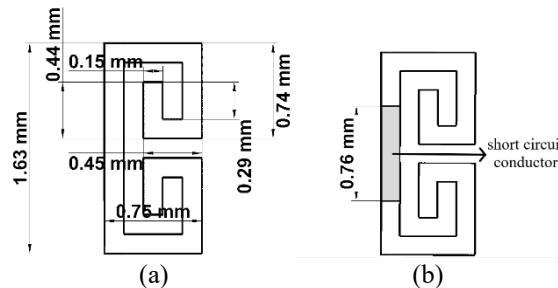

(a)   (b)

Fig. 2 - Modified Hairpin DGS layout for (a) active DGS (open circuit) and (b) inactive DGS (short circuit)

The DGS are implemented in the filter design, and Fig. 3's top and bottom views show the complete circuit structure for open circuited DGS. The DGS is placed underneath the transmission line in the ground plane.

In order to preserve the DGS independent of the layout ground, capacitors have been inserted adjacent to and beside it, as depicted in Fig. 3(a). Future designs must follow this procedure when PIN diode biasing is required for an automated switch among the filter's bandstop and allpass modes. As an RF choke, the radial stub that connects to the DGS's enclosed area prevents any radio wave from disrupting the PIN diode's biasing source.

The same setup was used for the filter design with shorted DGS. The microstrip line model mentioned in [20] was used to create both filters in EDA software. The use of a Rogers RT/Duroid 5880 substrate with a relative dielectric constant, ε_r of 2.2 and 0.254 mm thickness allowed for the realisation of convertible filters with ideal switch DGS. The performance of the filter design in terms of attenuation, insertion loss, and return loss was also simulated using the software.
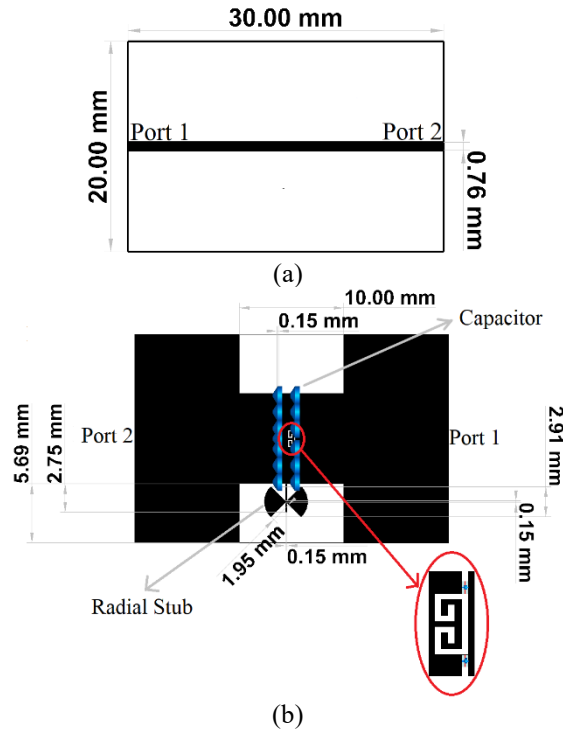
(a)

(b)

Fig. 3 - Convertible filter with the ideal switch DGS from (a) top view and (b) bottom view

4. Results and Discussion

The results of the convertible filter simulation utilising Hairpin DGS with ideal switches are shown in Fig. 4. The open circuit condition filter worked in the 26 GHz range, with a maximum attenuation level (S_{21}) of 29.5 dB and a 2.16 GHz attenuation response bandwidth at 10 dB level. Comparing the DGS circuit size to its original in [19], it is also small. The large attenuation magnitude and narrow bandwidth result can significantly increase the frequency selectivity of the filter. Additionally, the return loss (S_{11}) is lower than 2 dB, suggesting that the DGS has an impact on reverting the EM wave to its supply while boosting the bandstop characteristics of the filter. The short circuit state has rendered the filter's DGS effect inactive, resulting in a broadband allpass response that has an insertion loss (S_{21}) of roughly 0.5 dB and more than 10 dB of return loss (S_{11}).
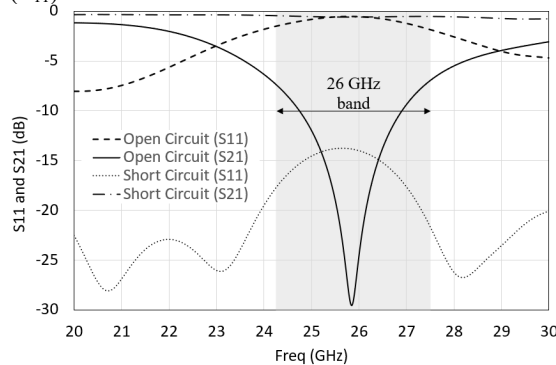

Fig. 4 - Simulated results of S11 and S21 for the filter with DGS in open circuit and short circuit conditions

The attenuation and insertion loss analyses in (6) and (7) are said to be consistent with the simulated results in Fig. 4, since the results demonstrated that high attenuation (approximately 30 dB as relative to ∞ dB) and relatively small insertion loss (around 0.5 dB as relative to 0 dB) were accomplished.

The outcomes of their electric field (E-field) pattern can likewise be analysed to characterise the S_{11} and S_{21} behavioural responses of the convertible filter for both open and short circuit conditions, as shown in Fig. 5. An open circuit condition results in a clearly centred E-field that is reflected back to the source, producing an outstanding bandstop filter response. The E-field, however, can be transmitted when a DGS filter has a short circuit situation, acting as an allpass filter.
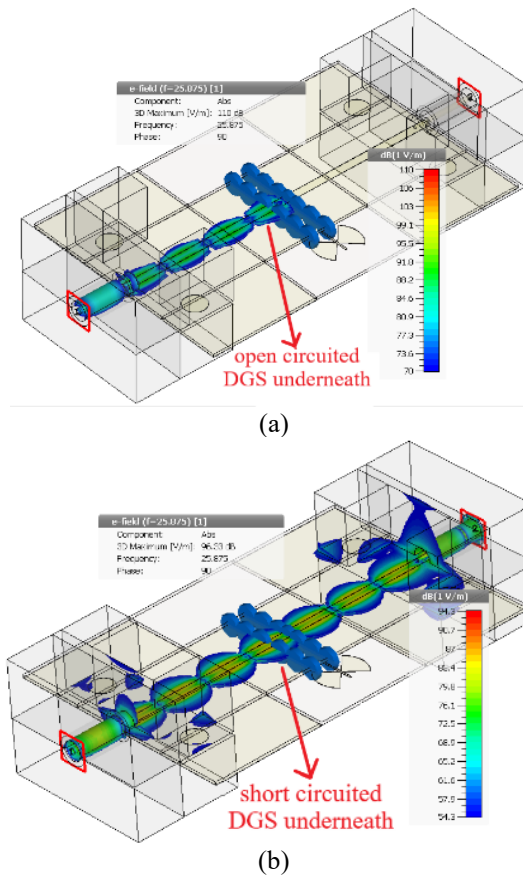
(a)

(b)

Fig. 5 - E-field pattern of the filter with the ideal switch DGS under the following two conditions: (a) open circuit and (b) short circuit

5. Conclusion

The simulation analysis satisfactorily indicates that the convertible filter utilising DGS may apply open circuit and short circuit conditions with an ideal switch to switch between bandstop and allpass responses. For the DGS during bandstop response with narrowband qualities, there is good agreement between the results of the mathematical and simulation assessments for S11 and S21. Additionally, the outcomes are calculated for an allpass response with wideband characteristics in the 26 GHz region when the DGS is shorted. To replace the ideal switch with real switching components, like PIN diodes, for practical applications in mm-wave 5G telecommunications, more research is required.

Acknowledgement

References

[1] D. Choudhury, "5G wireless and millimeter wave technology evolution: An overview," *2015 IEEE MTT-S International Microwave Symposium*, 2015, pp. 1-4.

[2] Y. Cho, H. -K. Kim, M. Nekovee and H. -S. Jo, "Coexistence of 5G with satellite services in the millimeter-wave band," in *IEEE Access*, vol. 8, pp. 163618-163636, 2020.

[3] Saleh, Mohammed Mehdi, Ahmed A. Abbas, and Ahmed Hammoodi. "5G cognitive radio system design with new algorithm asynchronous spectrum sensing." *Bulletin of Electrical Engineering and Informatics*, vol. 10, no. 4, pp. 2046-2054, 2021.

[4] O. H. Toma and M. López-Benítez, "Cooperative spectrum sensing: A new approach for minimum interference and maximum utilisation," *2021 IEEE International Conference on Communications Workshops (ICC Workshops)*, 2021, pp. 1-6.

[5] Tin, Phu Tran, Duy-Hung Ha, Pham Minh Quang, Nguyen Thanh Binh, and Nguyen Luong Nhat. "Performance of multi-hop cognitive MIMO relaying networks with joint constraint of intercept probability and limited interference." *Telkomnika*, vol.19, no. 1, pp. 44-50, 2021.

[6]   Sarma S.S., Hazra R. "Interference mitigation methods for D2D communication in 5G network." In: *Mallick P., Balas V., Bhoi A., Chae GS. (eds) Cognitive Informatics and Soft Computing. Advances in Intelligent Systems and Computing*, vol 1040. Springer, Singapore.

[7]   D. Siafarikas, E. A. Alwan and J. L. Volakis, "Interference mitigation for 5G millimeter-wave communications," *2018 IEEE International Symposium on Antennas and Propagation & USNC/URSI National Radio Science Meeting*, 2018, pp. 391-392.

[8]   H. Islam, S. Das, T. Bose and T. Ali, "Diode based reconfigurable microwave filters for cognitive radio applications: A review," in *IEEE Access*, vol. 8, pp. 185429-185444, 2020.

[9]   El Fatimi, Aziz, Seddik Bri, and Adil Saadi. "Reconfigurable ultra wideband to narrowband antenna for cognitive radio applications using PIN diode." *Telkomnika*, vol. 18, no. 6, pp. 2807-2814, 2020.

[10]   R. Kumar Nirala, "An overview on defected ground structure in aspect of microstrip patch antenna," *Int. J. Recent Innov. Trends Comput. Commun.*, vol. 6, no. 1, pp. 31–34, 2018.

[11]   M. Dhanashri, S. Salgare, M. Shamala, and R. Mahadik, "A review of defected ground structure for microstrip antennas," *Int. Res. J. Eng. Technol.*, vol. 2, no. 6, pp. 150–154, 2015.

[12]   A. Kumar and A. P. Singh, "Enhancement of the Performance Parameters of Microstrip Slotted Patch Antenna using Defected Ground Structure," Int. J. Eng. Trends Technol., vol. 60, no. 2, pp. 122–127, 2019, doi: 10.14445/22315381/IJETT-V60P217.

[13]   E. G. Ouf, E. A. F. Abdallah, A. S. Mohra, and H. M. S. Elhennawy, "Electronically switchable ultra-wide band/dual-band bandpass filter using defected ground structures," *Prog. Electromagn. Res. C*, vol. 91, pp. 83–96, 2019.

[14]   H. A. Mohamed, H. B. El-Shaarawy, E. A. F. Abdallah, and H. M. El-Hennawy, "Frequency-reconfigurable microstrip filter with dual-mode resonators using RF PIN diodes and DGS," *Int. J. Microw. Wirel. Technol.*, vol. 7, no. 6, pp. 661–669, 2015.

[15]   S. Fouladi, F. Domingue, and R. Mansour, "CMOS-MEMS tuning and impedance matching circuits for reconfigurable RF front-ends," in *Proceedings 2012 IEEE MTT-S International Microwave Symposium Digest*, 2012, pp. 1–3.

[16]   A. H. Jabire, A. Abdu, S. Saminu, A. M. Sadiq, and M. J. Adamu, "Isolation Frequency Switchable MIMO Antenna for PCS, WIMAX and WLAN Application," Elektr. J. Electr. Eng., vol. 18, no. 3, pp. 27–33, 2019, doi: 10.11113/elektrika.v18n3.178.

[17]   S. Riaz, X. Zhao, and S. Geng, "A frequency reconfigurable MIMO antenna with agile feedline for cognitive radio applications," Int. J. RF Microw. Comput. Eng., vol. 30, no. 3, pp. 1–9, 2020, doi: 10.1002/mmce.22100.

[18]   Weng, Li Hong, Yu-Chun Guo, Xiao-Wei Shi, and Xiao-Qun Chen. "An overview on defected ground structure." *Progress In Electromagnetics Research B*, vol. 7, pp. 173-189, 2008.

[19]   S.U. Rehman, A.F.A. Sheta, M.A. Alkanhal and R.S. Aziz, "Reconfigurable bandstop filter using defected ground structure (DGS)", *2013 Saudi International Electronics, Communications and Photonics Conference*, 2013, pp. 1-4.

[20]   D. M. Pozar, *Microwave Engineering*, 4th ed. Wiley, 2011.